Journal of Power Sources 193 (2009) 935–938

Contents lists available at ScienceDirect

Journal of Power Sources

journal homepage: www.elsevier.com/locate/jpowsour

Short communication

Growth of single-crystal α-MnO_2 nanotubes prepared by a hydrothermal route and their electrochemical properties

Wei Xiao, Hui Xia, Jerry Y.H. Fuh, Li Lu*

Department of Mechanical Engineering, National University of Singapore, 9 Engineering Drive 1, Singapore 117576, Singapore

ARTICLE INFO

Article history:
Received 28 December 2008
Received in revised form 5 March 2009
Accepted 17 March 2009
Available online 17 April 2009

Keywords:
Nanotube
Hydrothermal method
Energy conversion
Supercapacitor
Manganese dioxide

ABSTRACT

Single-crystal α-MnO_2 nanotubes are synthesized by a facile hydrothermal method without the assistance of a template, a surfactant and heat-treatment. The single-crystal α-MnO_2 nanotube electrode possesses a high specific capacitance with a good power capability. The excellent pseudo-capacitive properties are attributed to a nanotubular microstructure and a large tunnel cavity in the α-MnO_2 crystal structure. Single-crystal α-MnO_2 nanotubes with good electrochemical performance can be a promising candidate as supercapacitor materials.

1. Introduction

Supercapacitors (SCs) which feature a high specific power and a long cycle capability have received intensive attention in recent years [1]. Among all of the potential materials, manganese oxides have been investigated widely as they could serve as low-cost and environmental friendly materials to replace the widely used hydrous RuO_2 without compromising specific power and specific energy.

One-dimensional (1D) nanostructured materials have attracted great interest because of their unique physicochemical properties that arise from their high surface area, novel size effects, and significantly enhanced kinetics [2,3]. Currently, template synthesis is one of the most commonly used methods to fabricate 1D nanostructured materials [4,5]. This template-assisted synthesis method is not only tedious but also requires multiple synthesis steps, expensive templates, and corrosive chemical treatment. By comparison, the hydrothermal synthesis method has proved to be an efficient way to prepare 1D nanostructured materials [6]. In addition, micro-architectures can be tailored by adjusting the synthesis temperature, the processing time and pressure, and by selecting different solvents and concentrations.

One-dimensional nanostructured manganese oxides, in the form of nanowires, nanorods, nanobelts and nanoneedles, have been successfully prepared via hydrothermal methods [7–13]. By contrast, only a few studies on the hydrothermal preparation of 1D nanostructured manganese oxides in nanotubes have been reported [14,15]. Single-crystal β-MnO_2 nanotubes were reported [14] to be prepared successfully by a hydrothermal method through oxidizing $MnSO_4$ with $NaClO_3$ in the presence of an organic surfactant (poly(vinyl pyrrolidone)). More recently, single-crystal α-MnO_2 nanotubes were obtained by a facile hydrothermal treatment of $KMnO_4$ in hydrochloric acid solution [15]. The hydrothermal route featured a low synthesis temperature and no surfactants were required. Therefore, this method is employed in the present work to prepare MnO_2 nanotubes. The work focuses on the optimization of the microstructures and crystal structures of manganese dioxides in order to improve their supercapacitive properties.

2. Experimental

The processing route followed the procedure reported recently with minor modifications [15]. In the present synthesis, 0.608 g $KMnO_4$ and 1.27 ml HCl (37 wt.%) were added to 70 ml distilled water with stirring to form the precursor solution. After stirring, the solution was transferred to a Teflon-lined, stainless-steel autoclave with a capacity of 100 ml. The autoclave was kept in an oven at 140 °C for 12 h, and then cooled down to room temperature. The resulting brown precipitates were collected, rinsed and filtered to a pH 7. The as-prepared powders were then dried at 80 °C in air.

The crystal structures and microstructures of the products were characterized by means of X-ray diffraction (XRD, Shimadzu 6000, λ = 1.5405 Å), scanning electron microscopy (SEM, Hitachi, S-4300)

* Corresponding author. Tel.: +65 65162236; fax: +65 67791459.
E-mail address: luli@nus.edu.sg (L. Lu).

0378-7753/$ – see front matter © 2009 Elsevier B.V. All rights reserved.
doi:10.1016/j.jpowsour.2009.03.073

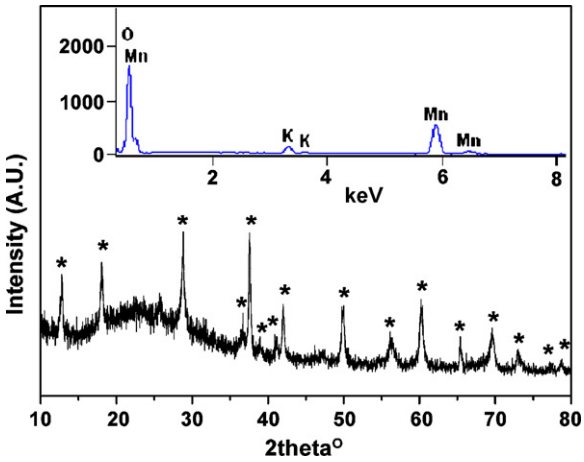

Fig. 1. XRD pattern and EDX spectrum (inset) of prepared MnO_2 nanotubes. (The *stars* denote the peaks of α-MnO_2, JCPDS: 44-0141.)

and transmission electron microscopy (TEM, JEOL3010) with energy dispersive X-ray (EDX) spectroscopy (Oxford) and selected area electron diffraction (SAED) accessories.

To measure the electrochemical performance of the as-synthesized MnO_2 nanotubes, the MnO_2 nanotubes (80 wt.%) was mixed with a binder (10 wt.%) (polytetrafluoroethylene) and acetylene black (10 wt.%). The mixture of the MnO_2 nanotubes was then rolled to form a uniform film that was vacuumed-dried at 120 °C for 12 h. A circular piece of the film (1 cm^2) was cut and pressed on nickel to form the working electrode. Weight of the electrode was measured by a balance (AND GR-202) with an accuracy of 0.01 mg. The exposed apparent surface area is 1 cm^2 and the typical loading of MnO_2 is about 0.5 mg.

All electrochemical tests were conducted in a one-compartment, three-electrode electrochemical bath which contained 1.0 M sodium sulfate aqueous solution as the electrolyte, a platinum foil (2 cm × 2 cm, Aldrich) as the counter electrode and an Ag|AgCl electrode (CHI111) as reference electrode. The electrochemical properties were examined by a Solartron SI1287 electrochemical Interface and a Solartron SI1260 Impedance Analyzer. The electrochemical impedance spectroscopy (EIS) was investigated at the

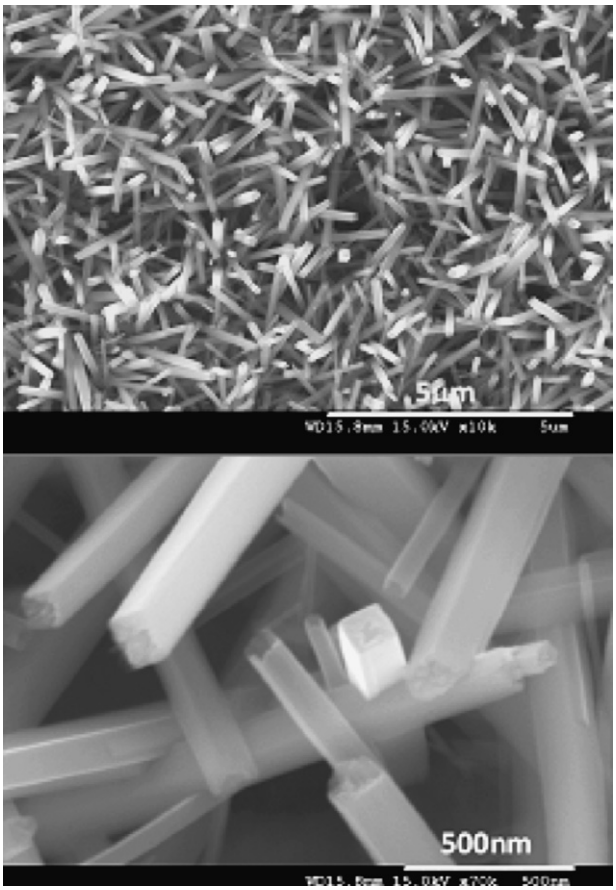

Fig. 2. SEM images of prepared MnO_2 nanotubes in different magnifications.

open-circuit potential over the frequency range of 10^5 to 0.1 Hz with an a.c. amplitude of 10 mV.

The charge, *Q*, was obtained by integration of area under the cyclic voltammetry (CV) plot, and the specific capacitance, *C*, was then deduced based the charge, the mass of the active materials, *m*,

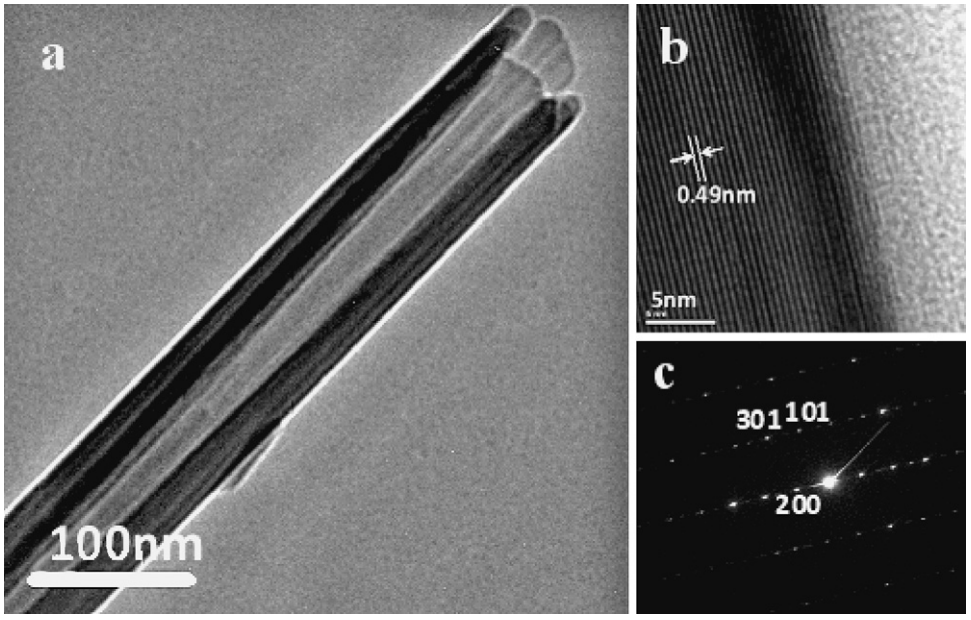

Fig. 3. (a) TEM, (b) HRTEM images and (c) SAED pattern of prepared MnO_2 nanotubes.

and the potential window, ΔV according to

$$C = \frac{Q}{2m \times \Delta V} \quad (1)$$

3. Results and discussion

The XRD spectrum of the as-synthesized MnO_2 is shown in Fig. 1. All the diffraction peaks can be indexed to the α-MnO_2 phase, and no other characteristic peaks from impurities are observed. This demonstrates the high purity of the sample. Generally, MnO_2 exists in several crystallographic phases, i.e., the α, β, γ, δ and λ forms. These phases are distinctive from each other because the basic unit [MnO_6] octahedra are linked in different ways [13]. Hence, different phases possess tunnels or interlayers with gaps of different magnitude. Structurally, α-MnO_2 is built from double chains of edge-sharing MnO_6 octahedra, which are linked at the corners to form $(2 \times 2)+(1 \times 1)$ tunnel structures that extend in a direction parallel to the *c* axis of the tetragonal unit cell. The (1×1) tunnels are generally empty because of their small size (1.89 nm). By contrast, the size of (2×2) tunnel is about 0.46 nm, which is suitable for insertion/extraction of alkali cations and is the reason for using α-MnO_2 as molecular/ion sieves [9,11–13,15]. During the synthesis process, some cations and water can be introduced into the tunnels from the precursors. The inset of Fig. 1 presents the EDX spectrum of the sample and shows the presence of potassium in the sample with a K:Mn atomic ratio of around 11.66%. The chemical composition of the sample derived from EDX analysis can be approximately denoted as KMn_8O_{16} and is consistent with the chemical composition of cryptomelane [11,12]. For the convenience of discussion, the synthesized K^+-containing α-MnO_2 is denoted as α-MnO_2 in the following discussion.

Scanning electron micrographs (SEMs) of the synthesized α-MnO_2 are shown in Fig. 2. From the low-magnification SEM, it can be seen that the panoramic morphology of synthesized α-MnO_2 powder consists of uniform 1-D nanostructured crystals without other morphologies in the sample. The high-magnification TEM image in Fig. 3a shows that the one-dimensional nanostructure has a tetragonal open end with an edge length of about 80 nm and a longitudinal length of several nm. The inner size is about 25 nm. The representative tubular structure of the products confirms the formation of nanotubes. An HRTEM image of the prepared α-MnO_2 nanotubes is presented in Fig. 3b. It shows clear lattice fringes along the nanotube, which confirms the nature of the single crystal of the synthesized α-MnO_2 nanotubes. A lattice spacing of 0.49 nm between adjacent planes in the image corresponds to the distance of the (2 0 0) planes in the tetragonal α-MnO_2 structure. A selected area electron diffraction (SAED) pattern taken from a single nanotube is shown in Fig. 3c. The SAED pattern and HRTEM analysis indicate that the nanotube axis is along the [0 0 1] direction (*c* axis) [15]. The TEM investigations shown in Fig. 3 confirm the high-quality single-crystalline features of the synthesized α-MnO_2 nanotubes.

Generally, two mechanisms are proposed for supercapacitive charge storage in MnO_2 [13]. The first mechanism is based on the intercalation/extraction of protons or alkali cations into the oxide particles (denoted as *reaction* (1) in Eq. (2)), whereas the second mechanism involves the surface adsorption/desorption of proton or alkali cations (denoted as *reaction* (2) in Eq. (3)):

$$MnO_2 + M^+ + e^- = MnOOM \quad (2)$$

and

$$(MnO_2)_{surface} + M^+ + e^- = (MnOOM)_{surface} \quad (3)$$

where M^+ denotes as Na^+, K^+ or H_3O^+.

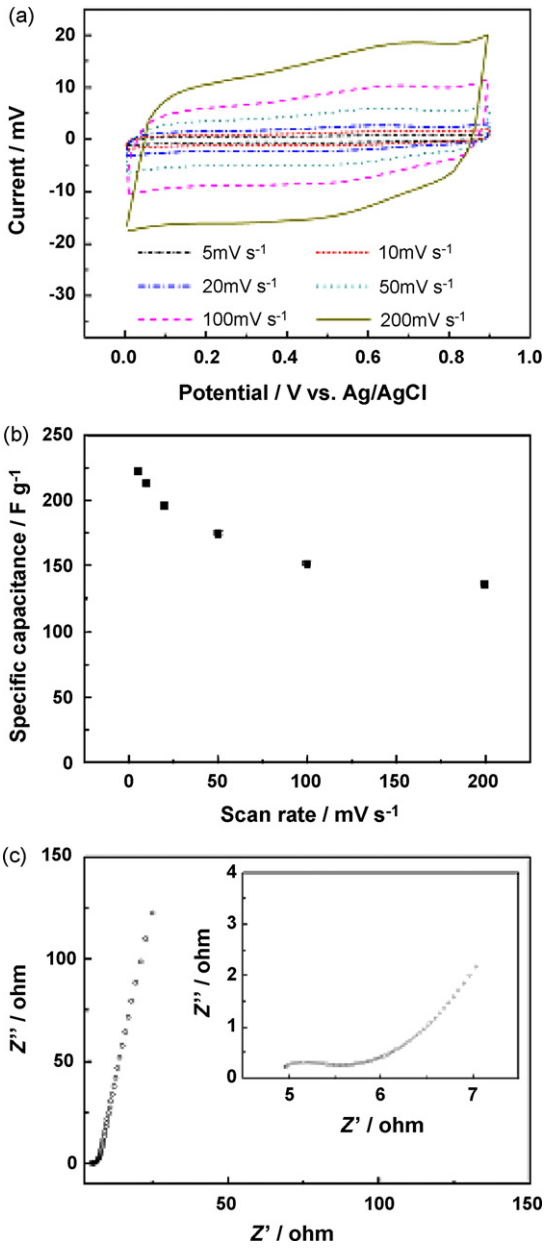

Fig. 4. (a) Cyclic voltammetric plots of MnO_2 nanotubes electrode at different scan rates; (b) specific capacitances of MnO_2 nanotubes electrode calculated from CVs in (a) against the scan rates; (c) Nyquist plot for MnO_2 nanotubes electrode.

The supercapacitive properties of prepared α-MnO_2 nanotubes were investigated by CV at different scan rates. The CV plots in Fig. 4a at all scan rates are close to a rectangular shape with a mirror-image feature. This indicates the excellent reversibility and ideal capacitive property of the electrode. The specific capacitance (SC) values calculated from Fig. 4 are 220, 213, 196, 175, 152 and 136 $F g^{-1}$ at scan rates of 5, 10, 20, 50, 100 and 200 $mV s^{-1}$, respectively. These data indicate the large specific capacitance and the good power capability of the synthesized α-MnO_2 nanotubes. The excellent supercapacitive properties of the synthesized α-MnO_2 nanotubes can be attributed to their unique microstructure and crystal structure. First, the nanotubular microstructure possesses extremely large surface area which enlarges electrode|electrolyte contact area and the surface adsorption–desorption of protons or alkali cations (*reaction* (2)). Second, the crystal structure of the synthesized single-crystal α-MnO_2 nanotubes is constructed from double chains of octahedral [MnO_6] which form the (2×2) tunnels

with a cavity as large as 0.46 nm. This large tunnel has the potential to contain different cations and to make the material attractive as electrodes in batteries and supercapacitors. For supercapacitive investigations, the large tunnels in the crystal structure of the synthesized single-crystal α-MnO_2 nanotubes enhance the intercalation/extraction of protons or alkali cations into the bulk of the oxides (*reaction* (1)). Last, but not least, the nanotubular microstructure shortens the diffusion distance for ions, and hence facilitates the power capability.

The electrochemical properties of the α-MnO_2 nanotube electrode were also studied by EIS. Fig. 4c shows a Nyquist plot with a semicircle in the high-frequency range, followed by a straight sloped line in the low-frequency region. The diameter of the semicircle corresponds to the interfacial charge-transfer resistance (R_{ct}), which is called the Faraday resistance and is often the limiting factor for the power density of a supercapacitor. The EIS pattern can be fitted by an equivalent circuit [9], and the calculated R_{ct} of the α-MnO_2 nanotube electrode is 0.95 Ω, which could significantly facilitate the power density of the electrode. The nearly ideal straight line along the imaginary axis at the lower frequencies indicates that the electrode has low diffusion resistance. The EIS results confirm the excellent electrochemical capacitive properties of the prepared α-MnO_2 nanotube electrode.

4. Conclusions

In summary, single-crystal α-MnO_2 nanotubes are synthesized by a facile hydrothermal method without the assistance of a template, a surfactant and heat-treatment. The single-crystal α-MnO_2 nanotube electrode shows a high specific capacitance with good power capability. Microstructure, crystal structure and electrochemical investigations confirm that the excellent supercapacitive properties are ascribed to the nanotubular microstructure and the crystal structure with a tunnel cavity as large as of 0.46 nm. Therefore, single-crystal α-MnO_2 nanotubes with good electrochemical performance could be promising candidate materials for supercapacitors.

Acknowledgements

The authors are grateful to the Agency for Science, Technology and Research of Singapore (A*Star) for financial support through grant R-284-000-067-597 and R-284-000-067-598 (072 133 0044), and to Dr. Zhang Zhen and Mr. Wang Hailong for useful discussions.

References

[1] P. Simon, Y. Gogotsi, Nat. Mater. 7 (2008) 845.
[2] J. Liu, G.Z. Cao, Z.G. Yang, D.H. Wang, D. Dubois, X.D. Zhou, G.L. Graff, L.R. Pederson, J.G. Zhang, ChemSusChem 1 (2008) 676.
[3] Y.G. Guo, J.S. Hu, L.J. Wan, Adv. Mater. 20 (2008) 2878.
[4] G.Z. Cao, D.W. Liu, Adv. Colloid Interf. Sci. 136 (2008) 45.
[5] S.J. Hurst, E.K. Payne, L.D. Qin, C.A. Mirkin, Angew. Chem. Int. Ed. 45 (2006) 2672.
[6] W.T. Yao, S.H. Yu, Int. J. Nanotechnol. 4 (2007) 129.
[7] F.Y. Cheng, J.Z. Zhao, W. Song, C.S. Li, H. Ma, J. Chen, P.W. Shen, Inorg. Chem. 45 (2006) 2038.
[8] X. Wang, Y.D. Li, Chem. Eur. J. 9 (2003) 300.
[9] M.W. Xu, L.B. Kong, W.J. Zhou, H.L. Li, J. Phys. Chem. C 111 (2007) 19141.
[10] V. Subramanian, H.W. Zhu, R. Vajtai, P.M. Ajayan, B.Q. Wei, J. Phys. Chem. B 109 (2005) 20207.
[11] Z.X. Liu, Y. Xing, C.H. Chen, L.L. Zhao, S.L. Suib, Chem. Mater. 20 (2008) 2069.
[12] T. Gao, M. Glerup, F. Krumeich, R. Nesper, H. Fjellvag, P. Norby, J. Phys. Chem. C 112 (2008) 13134.
[13] S. Devaraj, N. Munichandraiah, J. Phys. Chem. C 112 (2008) 4406.
[14] D.S. Zheng, S.X. Sun, W.L. Fan, H.Y. Yu, C.H. Fan, G.X. Cao, Z.L. Yin, X.Y. Song, J. Phys. Chem. B 109 (2005) 16439.
[15] J. Luo, H.T. Zhu, H.M. Fan, J.K. Liang, H.L. Shi, G.H. Rao, J.B. Li, Z.M. Du, Z.X. Shen, J. Phys. Chem. C 112 (2008) 12594.